Wave pattern and weak localization of chaotic versus scarred modes in stadium-shaped surface-emitting lasers

Y. T. Yu, P. H. Tuan, P. Y. Chiang, H. C. Liang, K. F. Huang, and Y. F. Chen*
Department of Electrophysics, National Chiao Tung University, 1001 Ta-Huseh Road, Hsinchu, 30050, Taiwan
(Received 17 May 2011; revised manuscript received 24 August 2011; published 3 November 2011)

We explore the lasing mode selection between the chaotic and scarred modes in stadium-shaped vertical-cavity surface-emitting lasers (VCSELs). Experimental results reveal that the spatial gain distribution in the active layer of a VCSEL can be modified via the aperture size to favor the generation of either the chaotic or the scarred modes. Experimentally obtained chaotic and scarred modes are further employed to perform statistical analysis of wave function intensities for making a comparison with predictions based on the nonlinear σ model. We verify that the scarring effect can be quantitatively relevant to the weak-localization correction in the intensity probability distribution.

DOI: 10.1103/PhysRevE.84.056201 PACS number(s): 05.45.Mt, 42.55.Px, 42.60.Jf, 73.20.Fz

I. INTRODUCTION

Current research in quantum chaos or wave chaos is mainly focused on wave function structure and transport in wave systems with a chaotic ray limit [1]. One of the most intriguing discoveries is the presence of scarred states that deviate significantly from a Gaussian random fluctuation by exhibiting a large excess of intensity near extraordinary unstable periodic orbits of the corresponding classical dynamics [2]. Since their theoretical discovery in a quantum framework, scars have been observed and predicted both experimentally and numerically in a wide variety of physical systems, including microwave cavities [3], Faraday surface waves [4], vibrating soap films [5], acoustic radiation [6], hydrogen atoms in a magnetic field [7], electrons in a resonant tunneling diode with a magnetic field [8], and molecular vibration [9].

The spatial structures of laser modes in broad-area resonators have received much interest for a long time because they give a deep insight into the pattern formation of natural waves [10–17]. Scarred modes have also been observed in microdisk lasers [18,19] and have been confirmed to possess the highest quality factors and high directionality. However, only a few efficient scarred modes can be supported in microdisk lasers because boundary losses played a critical role in the mode selection mechanism [20]. Moreover, the reimaging of lasing wave patterns on the vertical surface is a thorny subject due to the lateral radiation of microdisk lasers. The spatial patterns of lasing modes have significant value for exploring the statistical properties of wave function intensities in position space, which can be compared with the related theoretical model for verifying the presence of the scarring phenomenon.

In contrast to two-dimensional (2D) microdisk lasers, vertical-cavity surface-emitting lasers (VCSELs) have a dominant longitudinal wave vector k_z that makes it quite feasible to measure the spatial patterns of lasing modes with simple optics. Recently, the transverse modes of oxide-confined large-aperture VCSELs have been identified as novel emulations of the wave functions of 2D quantum billiards with the same confinement [21–23]. Even though the spatial gain distribution has been verified to play an important role in the usual optical resonators for the selective excitation of modes [24,25], its influence on mode selection in large-aperture VCSELs is still an open issue [26].

The spatial gain distribution of VCSELs is mainly determined by the oxide aperture size for a given operation temperature. To illustrate the influence of the aperture size, we use a distributed resistance network [27] to numerically analyze the carrier density distribution for VCSEL devices with mesa diameter of 140 μm and aperture diameters of 40 and 60 μm, respectively. As shown in Fig. 1, the carrier density of the very-large-aperture (60 μm) VCSEL is concentrated more in the neighborhood of the aperture boundary, compared with the 40 μm VCSEL. This result indicates that the aperture size considerably affects the spatial gain distribution and may be a functional parameter in mode selection. Inspired by this finding, we fabricated stadium-shaped VCSELs of different sizes to explore the scarring effect on the resonant modes and to further analyze the position-space wave function statistics in real devices. The experimental results reveal that chaotic modes and scarred modes can be effectively selected by use of different aperture sizes. Furthermore, we analyze the mode intensity statistics to make a comparison with predictions based on the nonlinear σ model [28,29]. Numerical analyses indicate that the intensity statistics of experimental scarred modes agree very well with the theoretical predictions for the weak-localization phenomenon.

II. EXPERIMENTAL RESULTS AND DISCUSSION

To investigate the influence of the aperture size on the lasing mode, we fabricated two categories of VCSELs with the same stadium shape but with different aperture sizes of 30×60 and 20×40 μm^2. The device structures of the oxide-confined VCSELs were similar to those described in [14]. The emission wavelengths of all VCSELs were approximately 808 nm. Figure 2 shows an optical microscope image of the device operated with an electric current under threshold current at room temperature. The bright region indicates the stadium-shaped pattern of spontaneous emission. The VCSEL device was placed in a cryogenic system with a temperature stability of 0.1 K in the range of 200–300 K. A power supply

*yfchen@cc.nctu.edu.tw

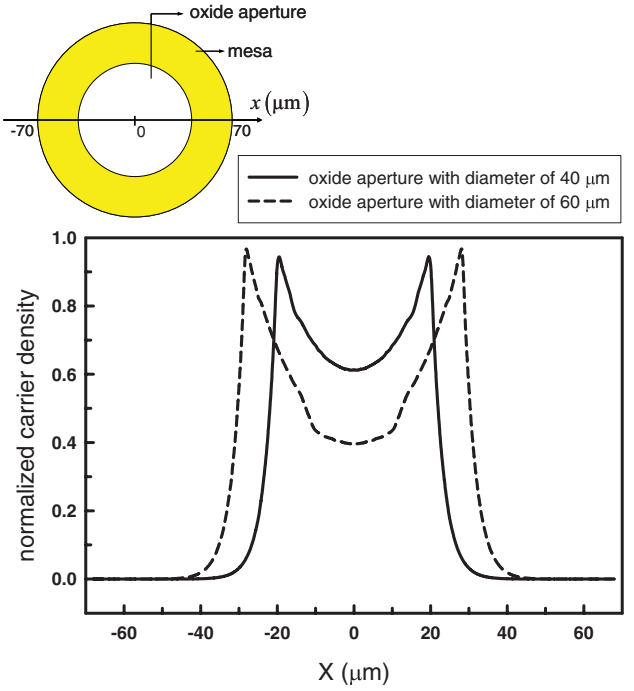

FIG. 1. (Color online) Calculated normalized carrier density in the active region of circular VCSELs with small (solid line) and large (dashed line) aperture size.

providing current with a precision of 0.01 mA was utilized to drive the VCSEL. The near-field patterns are measured by a charge-coupled device (CCD) camera (Coherent, Beam-Code) with an objective lens (Mitutoyo, numerical aperture 0.9). With thermal detuning, different transverse orders for the lasing modes can be generated.

First, we simulated the carrier density distribution in stadium-shaped VCSELs with different aperture sizes by using the distributed resistance network [27], as seen in Figs. 3(a) and 3(a′). As mentioned previously, the carrier density was distributed more nonuniformly in the large-aperture VCSEL than in the small one. We then observed the change of the lasing modes with operating temperature in the vicinity of the threshold for the stadium-shaped VCSEL with aperture size of $20 \times 40\ \mu m^2$. It was found that the lasing patterns exhibited morphologies like those of chaotic modes from low to high order when the operating temperature was changed from 280 to 200 K. Figures 3(b) and 3(c) depict the observed lasing patterns

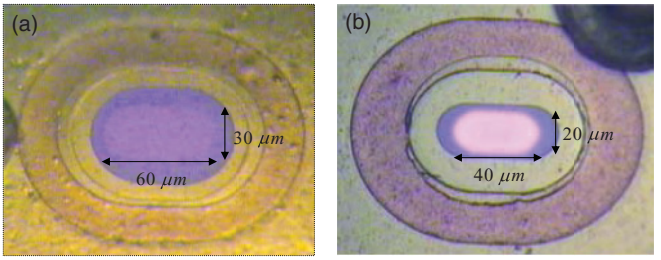

FIG. 2. (Color online) Schematics of stadium-shaped VCSEL device structure with aperture size of (a) $30 \times 60\ \mu m^2$, and (b) $20 \times 40\ \mu m^2$ which are measured with an optical microscope.

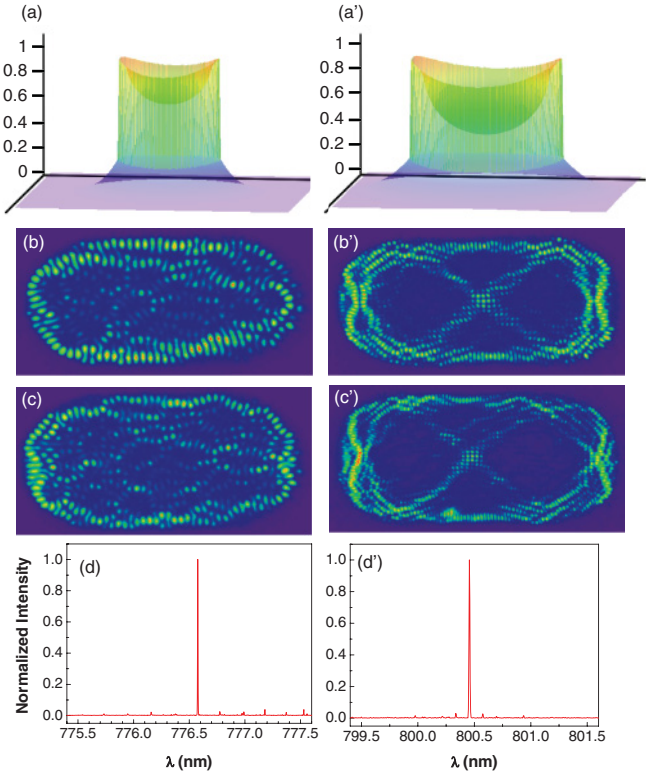

FIG. 3. (Color online) Calculated normalized carrier density in the active region of stadium-shaped VCSEL with (a) small aperture size and (a′) large aperture size. Observed lasing patterns for the stadium-shaped VCSEL of $20 \times 40\ \mu m^2$ at the device temperature of (b) 260 K and (c) 210 K and for the VCSEL of $30 \times 60\ \mu m^2$ at the device temperature of (b′) 260 K and (c′) 210 K. The emission spectra (d) and (d′) correspond to (c) and (c′), respectively.

at the operating temperatures of 260 K [Fig. 3(b)] and 210 K [Fig. 3(c)], respectively. More intriguingly, we found that the lasing patterns of the stadium-shaped VCSEL with the aperture size of $30 \times 60\ \mu m^2$ displayed spatial features like those of scarred modes from low to high order when the operating temperature was changed from 280 to 200 K. Figures 3(b′) and 3(c′) show the experimental lasing patterns at the operating temperatures of 260 K [Fig. 3(b′)] and 210 K [Fig. 3(c′)], respectively. It can be seen that the lasing patterns noticeably display the spatial localization on a double diamond structure. This is a realization of the scarred modes in stadium-shaped VCSELs based on the spatial gain nonuniformity arising from the aperture size. In brief, the aperture size actually affects the spatial gain distribution, leading to an effective mode selection between the chaotic and scarred modes. We also measured the emission spectra of these observed lasing patterns. We observed that both of them are single modes. Figures 3(d) and 3(d′) illustrate the experimental emission spectra which correspond to Figs. 3(c) and 3(c′).

III. STATISTICS OF EXPERIMENTAL WAVE PATTERNS

Although statistics of wave function intensities have been experimentally explored in the case of a diffusive billiard and have been compared with predictions based on the nonlinear σ model, such explicit analyses for chaotic and scarred modes in

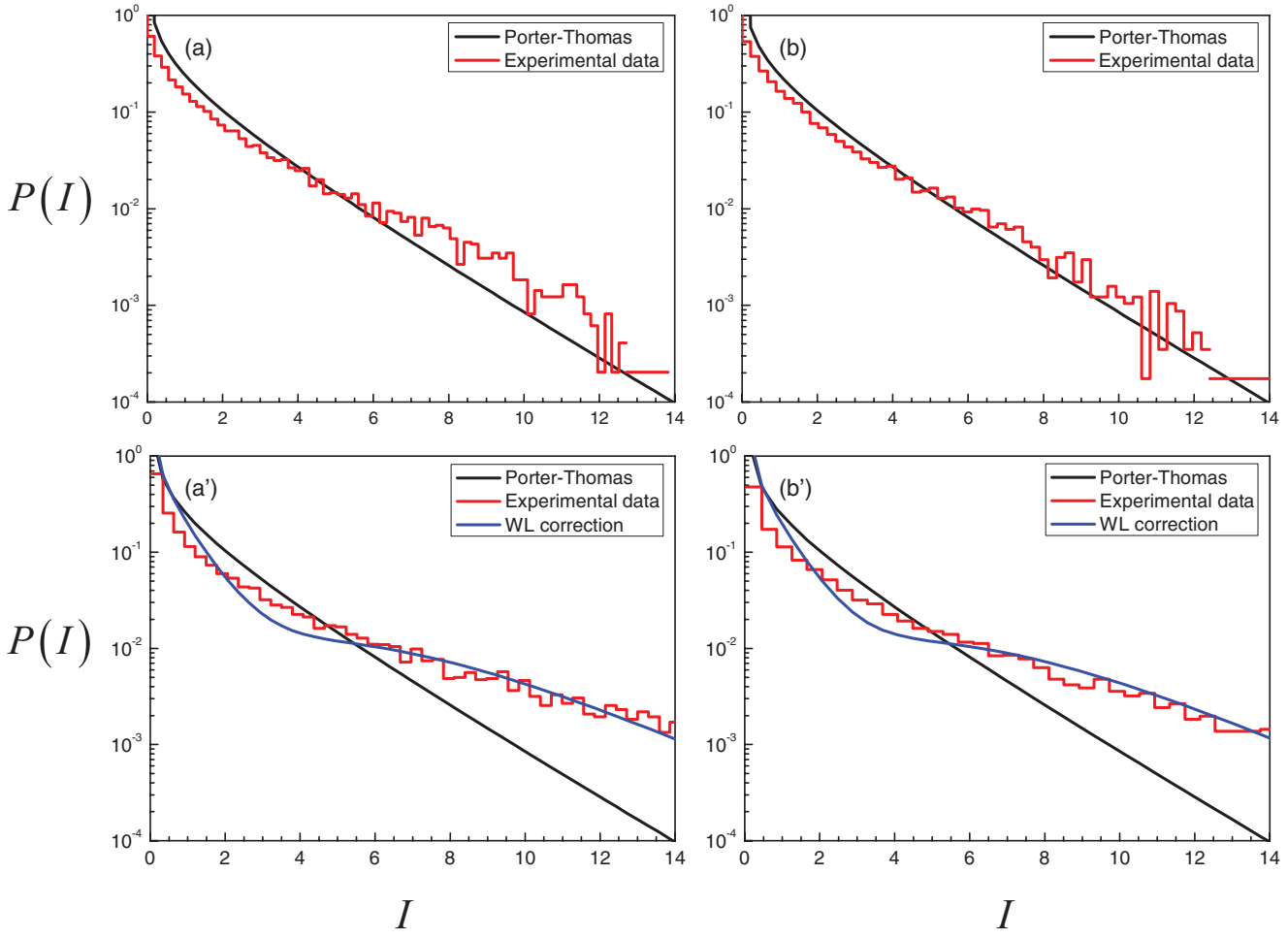

FIG. 4. (Color online) Intensity probability distribution $P(I)$ (a),(b) for the experimental chaotic modes shown in Figs. 3(b) and 3(c), respectively, and (a′),(b′) for the experimental scarred modes shown in Figs. 3(b′) and 3(c′), respectively. Black lines, Porter-Thomas (PT) distribution; blue lines, corrected distribution of Eq. (1). WL indicates weak localization.

the ballistic billiard are still lacking. Therefore, performing a statistical analysis for the observed chaotic and scarred lasing modes could provide real insight into the actual resonant wave function intensities. It is well known that the intensity statistics of theoretical chaotic wave functions are given by the classic Porter-Thomas (PT) distribution $P_{PT}(I) = \exp(-I/2)\sqrt{2\pi I}$ [30], where $I = |\Psi|^2$ and Ψ is the normalized wave function. Fyodorov and Mirlin [28,29] employed the nonlinear σ model to develop the relation for intensity statistics for the wave function with weak localization:

$$P_{FM}(I) = P_{PT}(I)\left[1 + (\langle I^2\rangle - 3)\left(\tfrac{1}{8} - \tfrac{1}{4}I + \tfrac{1}{24}I^2\right)\right], \quad (1)$$

where $\langle I^2\rangle = \int I^2 d^2r$ is the inverse participation ratio (IPR), which is a parameter manifesting the degree of localization. The universal value for the theoretical chaotic wave functions can be evaluated to be $\langle I^2\rangle = \int_0^\infty I^2 P_{PT}(I) dI = 3.0$. The IPR $\langle I^2\rangle$ is inversely proportional to the effective mode area. This result signifies that the IPR value for the scarred mode should be considerably larger than 3.0 and the mode with stronger scarring possesses a larger IPR value.

We numerically analyzed the observed lasing modes shown in Figs. 2 to acquire the intensity probability distribution. Figures 4(a) and 4(b) show the intensity probability distribution $P(I)$ for the experimental chaotic modes shown in Figs. 3(b) and 3(c), respectively. The theoretical PT distribution $P_{PT}(I)$ is also plotted in Figs. 4(a) and 4(b) for comparison, and fairly good agreement can be seen. Figures 4(a′) and 4(b′) show the intensity probability distribution $P(I)$ for the experimental scarred modes shown in Figs. 3(b′) and 3(c′), respectively. The IPR values for the experimental scarred modes shown in Figs. 3(b′) and 3(c′) are numerically found to be 5.08 and 5.34, respectively. By substitution of these IPR values into Eq. (1), the theoretical distributions with weak-localization correction, $P_{FM}(I)$, are calculated and depicted in Figs. 4(a′) and 4(b′) to make a comparison with the experimental results shown in Figs. 3(b′) and 3(c′), respectively. It is found that the intensity statistics for the experimental scarred modes are in good agreement with the corrected distributions $P_{FM}(I)$ but deviate from the PT distribution by different amounts. The good agreement confirms that the scarring effect can be quantitatively analyzed via the intensity probability distribution with weak-localization correction, $P_{FM}(I)$. We observe that this fit with the nonlinear σ model result works at the larger aperture, and also observe localization consistent with that fit, but the theoretical explanation must be left for

future work. Note that the lasing scarred modes are essentially related to the nonuniformity of carrier density distributions.

IV. CONCLUSIONS

In summary, we have experimentally confirmed that the aperture size can affect the spatial gain distribution in VCSELs and can be controlled to generate chaotic and scarred modes in stadium-shaped devices. Experimental results reveal that stadium-shaped VCSELs with aperture size of $20 \times 40\ \mu m^2$ have a comparatively uniform gain distribution and favor the generation of chaotic modes with spatially widespread patterns. In contrast, the stadium-shaped VCSELs with aperture size of $30 \times 60\ \mu m^2$ favor the generation of scarred modes with spatial patterns localized on a double diamond structure. We also employed experimental chaotic and scarred modes to perform a statistical analysis of wave function intensities and to compare the results with the predictions of the nonlinear σ model. It is confirmed that the scarring phenomenon can be quantitatively analyzed via the weak-localization effect in the intensity probability distribution.

ACKNOWLEDGMENT

The authors thank the National Science Council for their financial support of this research under Contract No. NSC-97-2112-M-009-016-MY3.

[1] S. W. McDonald, Lawrence Berkeley Laboratory Report No. LBL-14837, 1983 (unpublished).
[2] E. J. Heller, Phys. Rev. Lett. **53**, 1515 (1984).
[3] S. Sridhar, Phys. Rev. Lett. **67**, 785 (1991).
[4] A. Kudrolli, M. C. Abraham, and J. P. Gollub, Phys. Rev. E. **63**, 026208 (2001).
[5] E. Arcos, G. Baez, P. A. Cuatlayol, M. L. H. Prian, R. A. Mendez-Sanchez, and H. Hernandez-Saldana, Am. J. Phys. **66**, 601 (1998).
[6] D. Delande and D. Sornette, J. Acoust. Soc. Am. **101**, 1793 (1997).
[7] D. Wintgen and A. Hönig, Phys. Rev. Lett. **63**, 1467 (1989).
[8] P. B. Wilkinson, T. M. Fromhold, L. Eaves, F. W. Sheard, N. Miura, and T. Takamasu, Nature (London) **380**, 608 (1996).
[9] F. J. Arranz, F. Borondo, and R. M. Benito, Phys. Rev. Lett. **80**, 944 (1998).
[10] M. Brambilla, F. Battipede, L. A. Lugiato, V. Penna, F. Prati, C. Tamm, and C. O. Weiss, Phys. Rev. A **43**, 5090 (1991).
[11] D. Dangoisse, D. Hennequin, C. Lepers, E. Louvergneaux, and P. Glorieux, Phys. Rev. A **46**, 5955 (1992).
[12] E. Louvergneaux, D. Hennequin, D. Dangoisse, and P. Glorieux, Phys. Rev. A **53**, 4435 (1996).
[13] E. Louvergneaux, G. Slekys, D. Dangoisse, and P. Glorieux, Phys. Rev. A **57**, 4899 (1998).
[14] S. P. Hegarty, G. Huyet, J. G. McInerney, and K. D. Choquette, Phys. Rev. Lett. **82**, 1434 (1999).
[15] Y. F. Chen and Y. P. Lan, Phys. Rev. A **66**, 053812 (2002).
[16] F. Encinas-Sanz, S. Melle, and O. G. Calderón, Phys. Rev. Lett. **93**, 213904 (2004).
[17] E. Cabrera, O. G. Calderón, S. Melle, and J. M. Guerra, Phys. Rev. A **73**, 053820 (2006).
[18] C. Gmachl, F. Capasso, E. E. Narimanov, J. U. Nöckel, A. D. Stone, J. Faist, D. L. Sivco, A. Y. Cho, Science **280**, 1556 (1998).
[19] M. Lebental, J. S. Lauret, J. Zyss, C. Schmit, and E. Bogomolny, Phys. Rev. A **75**, 033806 (2007).
[20] W. Fang, H. Cao, and G. S. Salomon, Appl. Phys. Lett. **90**, 081108 (2007).
[21] K. F. Huang, Y. F. Chen, H. C. Lai, and Y. P. Lan, Phys. Rev. Lett. **89**, 224102 (2002).
[22] T. Gensty, K. Becker, I. Fischer, W. Elsäßer, C. Degen, P. Debernardi, and G. P. Bava, Phys. Rev. Lett. **94**, 233901 (2005).
[23] C. C. Chen, Y. T. Yu, Ross C. C. Chen, Y. J. Huang, K. W. Su, Y. F. Chen, and K. F. Huang, Phys. Rev. Lett. **102**, 044101 (2009).
[24] C. Vanneste, and P. Sebbah, Phys. Rev. Lett. **87**, 183903 (2001).
[25] J. Andreasen, C. Vanneste, L. Ge, and H. Cao, Phys. Rev. A. **81**, 043818 (2010).
[26] T. Ackemann, S. Barland, M. Cara, S. Balle, J. R. Tredicce, R. Jäger, M. Grabherr, M. Miller, and K. J. Ebeling, J. Opt. B: Quantum Semiclass. Opt. **2**, 406 (2000).
[27] R. Michalzik and K. J. Ebeling, IEEE J. Quantum Electron. **29**, 1963 (1993).
[28] Y. V. Fyodorov and A. D. Mirlin, Phys. Rev. B. **51**, 13403 (1995).
[29] A. D. Mirlin, Phys. Rep. **326**, 259 (2000).
[30] C. E. Porter and R. G. Thomas, Phys. Rev. **104**, 483 (1956).